Journal of Zoological Systematics and Evolutionary Research

WILEY

RESEARCH ARTICLE OPEN ACCESS

An Integrative Appraisal of the Diversity of the Genus *Myotis* (Chiroptera, Vespertilionidae) in Chile

Enrique Rodríguez-Serrano[1] | Belén Veloso-Frías[1,2] | Nicolás Espinoza-Aravena[1,3] | Kateryn Pino[1,3,4] | R. Eduardo Palma[5,6] | Cristián E. Hernández[3] | Ignacio Fernández-Latapiat[7] | Fulgencio Lisón[2,8]

[1]Laboratorio de Mastozoología, Departamento de Zoología, Facultad de Ciencias Naturales y Oceanográficas, Universidad de Concepción, Casilla 160-C, Concepción, Chile | [2]Wildlife Ecology and Conservation Lab, Departamento de Zoología, Facultad de Ciencias Naturales y Oceanográficas, Universidad de Concepción, Casilla 160-C, Concepción, Chile | [3]Facultad de Medicina Veterinaria, Universidad San Sebastián, Lientur 1457, Concepción, Chile | [4]Museo de Historia Natural, Universidad Nacional de San Agustín de Arequipa, Arequipa, Peru | [5]Universidad de O'Higgins, Avenue Libertador Bernardo O'Higgins 611, Rancagua, Chile | [6]Facultad de Ciencias Biológicas, Pontificia Universidad Católica de Chile, Avenue Libertador Bernardo O'Higgins 340, Santiago, Chile | [7]Myotis Chile SpA, Ñuñoa, Chile | [8]Ecosistemas Mediterráneos (ECOMED), Departamento de Ecología e Hidrología, Facultad de Biología, Universidad de Murcia, Campus de Espinardo, Murcia 30100, Spain

Correspondence: Enrique Rodríguez-Serrano (enrodriguez@udec.cl)

Received: 22 January 2026 | **Revised:** 16 March 2026 | **Accepted:** 31 March 2026

Academic Editor: Xiuguang Mao

Keywords: Atacama Desert | bat biodiversity | biogeography | Neotropical mammals | phylogenomics | species delimitation | temperate forest

ABSTRACT

The taxonomy of Chilean *Myotis* has long been contentious, particularly regarding the status of *M. arescens* relative to *M. atacamensis* and *M. chiloensis*. Here, we use an integrative framework combining genome-wide single nucleotide polymorphisms (SNPs), morphometrics, and bioacoustics to reassess lineage boundaries and evolutionary relationships in Chilean *Myotis*. We analyzed 19,707 high-quality SNPs from 80 specimens spanning the full latitudinal distribution of the group, 10 external and craniodental measurements from 123 specimens, and 825 echolocation pulses from free-flying bats. Population genomic analyses revealed three genetic clusters, but only *M. atacamensis* formed a deeply divergent and well-supported lineage, with no detectable recent gene flow to southern taxa. In contrast, *M. arescens* and *M. chiloensis* showed shallow genetic differentiation, strong asymmetric gene flow, and a latitudinal gradient of shared ancestry. Phylogenetic reconstruction based on SNPs failed to recover reciprocal monophyly between *M. arescens* and *M. chiloensis*, and process-based species delimitation strongly supported a two-lineage model comprising *M. atacamensis* and a single southern lineage (*M. chiloensis* + *M. arescens*). Morphometric and bioacoustics analyses mirrored these patterns: *M. atacamensis* was clearly differentiated in skull size and echolocation calls, whereas *M. arescens* and *M. chiloensis* formed overlapping morpho-acoustic continua. Together, our results indicate that *M. atacamensis* is an independently evolving desert-adapted lineage, while *M. arescens* represents a northern population within a geographically structured *M. chiloensis*. We therefore recommend recognizing only two *Myotis* species in Chile and interpreting *M. arescens* as a population-level unit within *M. chiloensis*, with important implications for taxonomy, biogeography, and conservation assessments.

1 | Introduction

The genus *Myotis* Kaup, 1829 (Chiroptera: Vespertilionidae) is nearly cosmopolitan, occurring on all continents except Antarctica. It represents one of the most speciose genera among mammals, with roughly 140 recognized species, including about 15 found in South America [1]. Despite this remarkable diversity, interspecific

phenotypic differentiation is often subtle, making species identification and delimitation particularly challenging. Consequently, morphological studies, especially those based on cranial and mandibular measurements, have played a central role in distinguishing taxa, given their association with trophic ecology, echolocation call design, and other functional traits [2]. Yet, the coexistence of morphological conservatism and cryptic genetic diversity has produced long-standing taxonomic and biogeographic ambiguities within the genus, with important implications for conservation assessments.

In Chile, the genus *Myotis* has historically received limited attention, largely due to its low species richness, narrow endemism, and the scarcity of genetic or morphometric studies [3]. Consequently, several competing hypotheses have arisen concerning species boundaries. Early taxonomic treatments by Cabrera [4] recognized three species (localities given after the author citation correspond to the type locality): *M. chiloensis* (Waterhouse and Darwin [5]; according to Waterhouse and Darwin: islets on the eastern side of Chiloé Island), *M. atacamensis* (Lataste [6]; San Pedro de Atacama), and *M. gayi* (Lataste [6]; Valdivia). The validity of *M. gayi* was soon questioned, as it lacked diagnostic characters to justify species status while not fitting clearly within *M. chiloensis*. Osgood [7] later described *M. chiloensis arescens* from Limache, near Valparaíso, and regarded both *M. atacamensis* and *M. gayi* as subspecies of *M. chiloensis*, thus recognizing a single species in Chile. Subsequent revisions alternately split or merged these taxa: LaVal [8] revalidated *M. atacamensis* as distinct, whereas Mann [9] considered three subspecies under *M. chiloensis* (*M. c. chiloensis*, *M. c. atacamensis*, and *M. c. arescens*). Later molecular analyses placed *M. atacamensis and M. chiloensis* on distant branches within the Neotropical *Myotis* phylogeny: *M. atacamensis* clustering with northern South American taxa and *M. chiloensis* with Andean and southern South American species [3]. More recently, Morales et al. [10], using 1610 ultraconserved elements, established that *M. chiloensis* is sister to a clade comprising *M. levis*, *M. nigricans*, *M. caucensis*, *M. oxyotus*, and the subclade *M. atacamensis* + *M. martiniquensis*, thus strongly supporting the presence of two *Myotis* species in Chile. Nevertheless, the taxonomic status of *M. c. arescens* has remained ambiguous, being alternately regarded as a synonym or subspecies of *M. chiloensis* [11–17].

More recently, Novaes et al. [1] revisited the taxonomy of Chilean *Myotis* through an integrative analysis combining mitochondrial molecular, morphological, and bioacoustic evidence. They recognized *M. arescens* [7] as a valid species, distinct from both *M. atacamensis* and *M. chiloensis*, thereby establishing a clearer taxonomic and geographic framework for the Chilean representatives of the genus. Nevertheless, their sampling was geographically uneven, lacking specimens from several key regions, particularly those corresponding to potential contact zones between the putative species. As a result, interpretations regarding morphological differentiation and species distributions remain tentative and require further evaluation.

To address these shortcomings, we conducted a re-evaluation of the *Myotis* complex in Chile using an expanded latitudinal sampling strategy. Our approach emphasizes morphological analyses in an explicit geographical scenario and is complemented by bioacoustic data, the latter providing potential additional diagnostic traits in taxa characterized by morphological conservatism. Furthermore, to overcome the limitations associated with low phenotypic and molecular variability and to resolve taxonomic ambiguities with higher precision, we incorporated genomic evidence based on single nucleotide polymorphisms (SNPs). SNPs have emerged as a powerful tool for delineating cryptic species, quantifying gene flow, and reconstructing evolutionary histories with unprecedented resolution [18, 19]. In bat systematics, genome-wide SNP datasets have revealed fine-scale population structure and clarified species boundaries where traditional markers proved inconclusive [20, 21]. For instance, recent genomic analyses of North American and European *Myotis* species have uncovered hidden lineages and refined long-debated taxonomic relationships (e.g., [22, 23]). By integrating morphological, bioacoustic, and genomic perspectives, our study aims to provide a comprehensive and robust understanding of the diversity, geographic structure, and evolutionary relationships of *Myotis* in Chile.

2 | Materials and Methods

2.1 | Sampling and DArTseq Sequencing

We sampled a total of 80 specimens obtained from field work (Supporting Information 1: Table S1 [table of genotyped specimens used in this study] Ethics Committee Approval from Universidad de Concepción N°CEBB 1175-2022; Servicio Agrícola y Ganadero, Ministerio de Agricultura, Gobierno de Chile Collecting Authorization N°3024/2022) and from the Instituto de Salud Pública de Chile, Ministerio de Salud, Gobierno de Chile. These samples represent three nominal species currently recognized in Chile, whose a priori assignment, following Novaes et al. [1], as *M. atacamensis* ($n = 9$) from Arica (18°28′33.24″ S) to Vallenar (28°34′35.04″ S), *M. arescens* ($n = 50$) from La Serena (29°53′43.08″ S) to Villarrica (39°16′57″ S), and *M. chiloensis* ($n = 21$) from Panguipulli (39°39′15.12″ S) to Seno Almirantazgo (54°28′35.4″ S) (Figure 1B; Supporting Information 2: Figure S1; Supporting Information 1: Table S1).

DNA extraction, high-coverage sequencing, and SNP genotyping were performed by Diversity Arrays Technology Pty Ltd (Canberra, Australia) using the DArTseq pipeline [24]. SNPs were called using *Eptesicus fuscus* (GCA_027574615.1, [25]) and *Myotis yumanensis* (GCA_028538775.1; [26]).

Data filtering was conducted in *dartR* v2.9.9.5, removing SNPs with reproducibility below 0.95, missing from more than 70 % of samples, occurring in the same fragment as other SNPs (to avoid linkage), or monomorphic loci. We also excluded loci deviating from Hardy–Weinberg equilibrium ($\alpha = 0.05$) and those whose minor allele occurred in a single individual. The final dataset comprised 19,707 high-quality SNPs (data available at https://doi.org/10.5281/zenodo.18237365).

2.2 | Lineage Detection, Geographical Structure, Genetic Diversity, and Migration Rates

Genetic diversity within each *Myotis* species was summarized using the function *gl.basic.stats* implemented in *dartR*, which computes observed heterozygosity (H_O), expected heterozygosity (H_E), and the inbreeding coefficient (F_{IS}) for every locus and population (= species). Mean values of these indices were calculated per species to characterize overall genetic variation. Genetic

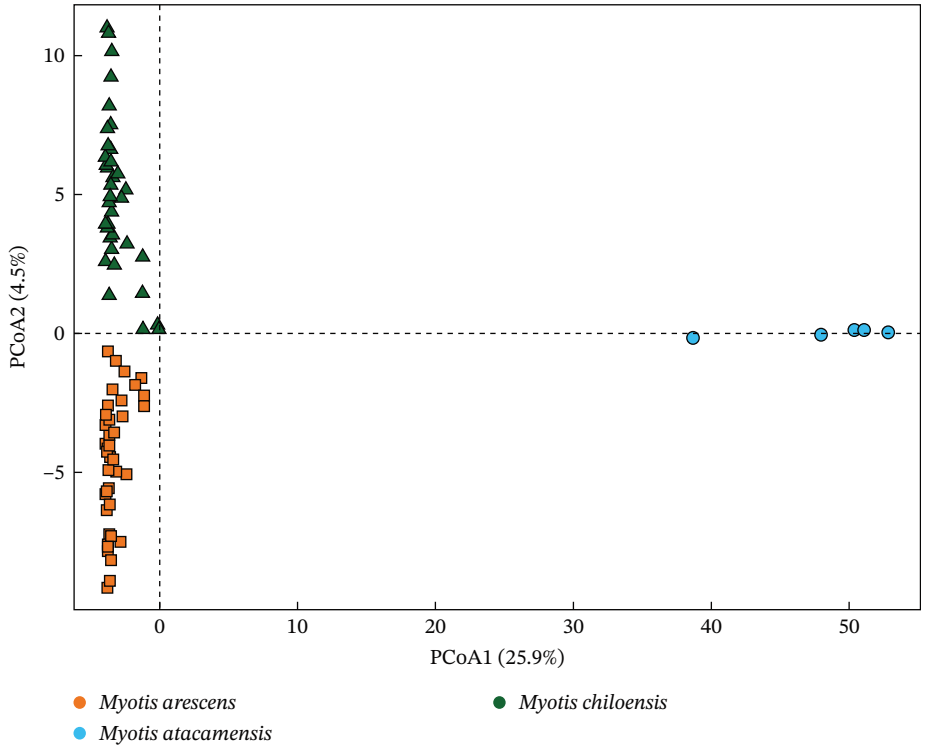

(A)

FIGURE 1 | (Continued)

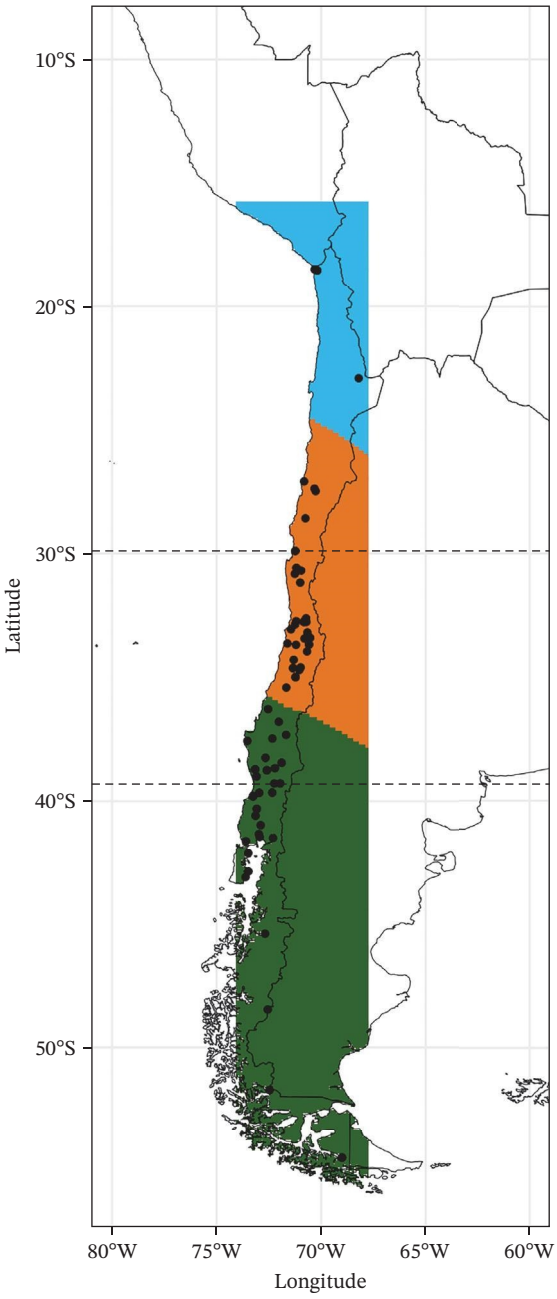

(B)

FIGURE 1 | (Continued)

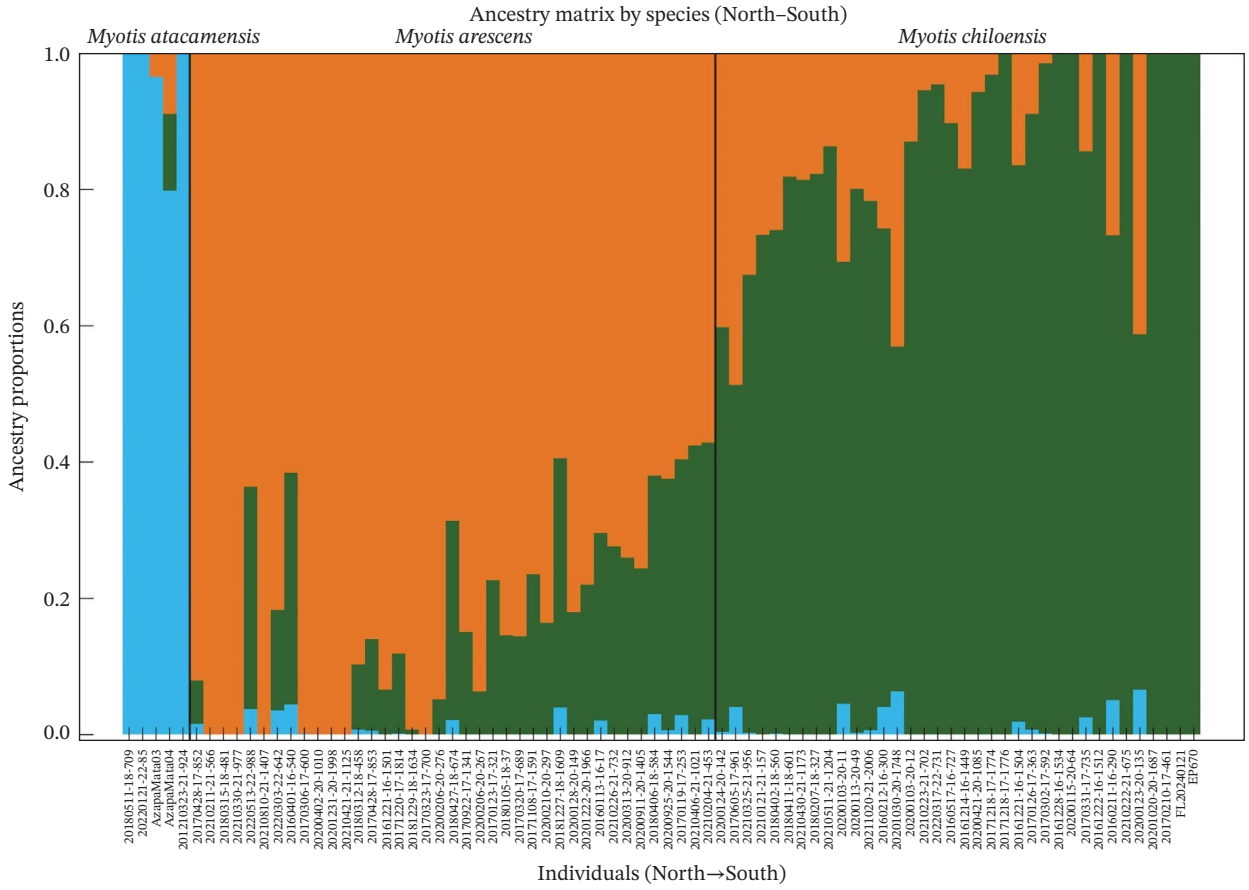

(C)

FIGURE 1 | Combined results of genetic diversity and ancestry for Chilean *Myotis*. (A) Principal coordinate analysis of 80 *Myotis* genotypes showing two species. (B) Spatial gradients representing the probability of occurrence for each of the three inferred ancestral populations, derived from ancestry matrix values. Dotted lines are the distribution limits proposed by Novaes et al. [1]. (C) Bar plot from ancestry analysis for $K = 3$, using a sparse non-negative matrix factorization approach. The specimens are arranged latitudinally on the *x*-axis (as in Supporting Information 1: Table S1).

differentiation among population (= species) was assessed with *gl.fst.pop* using the Weir and Cockerham [27] estimator and 1000 bootstrap replicates to obtain confidence intervals for pairwise and global F_{ST} values. Together, these analyses provide a comprehensive assessment of within- and among-species genetic structure in Chilean *Myotis*. These analyses were conducted under two alternative population assignment scenarios: a priori assignment following Novaes et al. [1] and a posteriori ancestry–based assignment.

To explore the genetic structure, we performed a principal coordinate analysis (PCoA) based on the SNP dataset. Patterns of genetic differentiation were evaluated using individual-based estimates of pairwise genetic and geographic distances to test for isolation by distance (IBD). Genetic distances among individuals were calculated using the bitwise distance metric [28] implemented in the R package *poppr* [29]. This distance measures the proportion of loci that differ between two multilocus genotypes while accounting for missing data and is optimized for high-throughput SNP datasets. Geographic distances were computed as great-circle (Haversine) distances in kilometers between sampling localities using the function *distm* from the R package *geosphere* [30]. Mantel tests were then performed to evaluate correlations between genetic and geographic distance matrices (9999 permutations; Pearson correlation) using the *mantel* function in the package *vegan* [31]. Two analyses were conducted: (1) a global test including all individuals of *M. atacamensis*, *M. arescens*, and *M. chiloensis* and (2) a focused test restricted to *M. arescens* and *M. chiloensis* to evaluate potential IBD patterns within this southern group. The relationship between genetic and geographic distances was visualized using scatter plots with linear regressions and Mantel coefficients (r, R^2, and p-values) for each analysis (Supporting Information 2: Figure S3). To further assess population differentiation and the presence of independently evolving lineages, we conducted an ancestry analysis using a sparse non-negative matrix factorization (sNMF) approach implemented in the R package *LEA* [32]. One hundred replicates were run for each number of ancestral populations (from $K = 1$ to $K = 10$), and the optimal $K = 3$ was selected according to the lowest cross-entropy value (Supporting Information 2: Figure S1A). Ancestry coefficients (Q matrix) were visualized as barplots and spatially interpolated according to the geographic coordinates of each sample using the R package *tess3r* [33]. The patterns of contemporary migration were analyzed using the software BayesAss3-SNPs [34], a modification of BayesAss version 3.0 [35] that allows handling large datasets. This software employs a Bayesian framework to estimate recent immigration rates based on

multilocus genotypes. We followed the strategy of grouping genotypes according to the population assignment provided by the ancestry analysis for the three focal species. Aiming for the acceptance rates (0.2–0.4), we set the mixing parameters for the inbreeding coefficient and allele frequencies to 0.10 and 0.30, respectively. Each analysis was run for 30,000,000 iterations, including a burn-in of 500,000 iterations, with samples recorded every 5000 iterations. The procedure was repeated five times using different random seed values. Convergence was assessed in TRACER V1.7.2 [36], both by visual inspection of the Markov chain states and by verifying that the estimated effective sample size exceeded 300. Median migration rates from the five independent runs were then used to build 95% credible intervals. The significance of migration rates was determined when the confidence intervals did not overlap with zero.

2.3 | Phylogeny and Species Delimitation Test

We use the complete database generated for lineage detection, geographical structure, and genetic diversity to generate a *fasta* archive. With this, we inferred the phylogenetic hypothesis of Chilean *Myotis* relationships under the maximum likelihood (ML) criterion using IQTREE 3 [37]. We performed an analysis without partitions. The best-fit nucleotide substitution model was selected by the *ModelFinder* algorithm (−m MF), under the Bayesian inference criterion (BIC). In addition, we perform a full tree search for every model (−mtree) to get an accurate analysis. We obtained the ML tree using a search of 1000 iterations (−1000), without constraint nodes, and support analysis using 1000 replicates of nonparametric bootstrap (−b 1000). We fixed the seed in 999 (−seed 999) to generate a reproducible analysis.

Considering the nature of the data in this work and the potential scenarios for the origin of Chilean *Myotis* species, we used a process-based approach to delimit independently evolving genealogical units [38]. Specifically, there is insufficient evidence to establish that southern South American *Myotis* species originated through allopatric processes, especially considering that various authors have treated these forms as subspecies associated with the climatic diversity of the enormous Chilean latitudinal gradient without abrupt breaks [39]. Consequently, population-level processes other than postisolation divergence, which would be expected in an allopatric model, should be more relevant in this scenario over thousands of kilometers of distribution, such as gene flow between divergent populations, the founder effect, with the consequent drastic change in population sizes, and others [38]. For this analysis, a database was created considering a balanced design (*M. atacamensis* = 5, *M. arescens* = 10, and *M. chiloensis* = 10) of specimens of the three nominal species and a sampling at each degree of latitude along the distributional range of these species to overcome the problems of previous studies. For this purpose, the specimens were chosen randomly according to these two criteria. We established the following five models: All putative species present gene flow between each other; only the forms *M. chiloensis* and *M. arescens* present flow; and all are independent units with historical or recent gene flow. We evaluated the parameters of each model and their fits in *delimitR* (Smith and Carstens [38]; Supporting Information 2: Figure S5). The divergence time between *M. atacamensis* and *M. chiloensis*/*M. arescens* was set at 11.8 Ma [10] and the generation time at 1.2 years according to the value estimated for the genus by Bhak et al. [40]. To assess the sensitivity of *delimitR* model selection to divergence-time uncertainty, we repeated the analyses using alternative divergence-time values of 10, 13, and 15 Ma around the estimate reported by Morales et al. [10]. The best model was selected according to its goodness of fit with model votes based on [38].

2.4 | Morphometric Analyses

To analyze the morphological variability of the nominal forms under study, we used 123 *Myotis* specimens, including the 78 (98% of correspondence) specimens from which the SNPs were obtained (Supporting Information 3: Table S2 [table of specimens used for morphological analyses]). Ten measurements (in mm) were obtained using a Mitutoyo caliper (0.01 mm) and a Zeiss graduated ocular (0.01 mm). We use one body and nine craniodental measurements, according to Horáček et al. [41]: forearm (FA) length of the FA from the elbow to the wrist; interorbital breadth (IOB) least breadth between the orbits; breadth across canines (BAC) greatest breadth across outer edges of the crowns of upper canines, including cingulae; breadth across molars (BAM) greatest breadth across outer edges of the crowns of upper molars; maxillary toothrow length (MTL) from the upper canine to M3; molariform toothrow length (M1–3) from M1 to M3; height of the coronoid process (HPC) measured in a line perpendicular to the main axis of the dentary excluding the angular process; mandible length (LMD) from the symphysis to the angular process; length of the lower toothrow (Li1–M3) between the first incisor and the third molar; and mandible height (HMD) measured on the mesial surface of the canine (Supporting Information 3: Table S2). We conducted a principal component analysis (PCA) using the *base* packages in R [42] to identify overall patterns of variation in the measurements. A canonical discriminant analysis (CDA) was then carried out with the *candisc* package [43] to compare shape and size among all *Myotis* samples. To quantify the discriminatory power of cranial morphology among taxa, we complemented the CDA with a leave-one-out cross-validation (LOOCV) procedure based on linear discriminant analysis. Classification success was evaluated as the proportion of specimens correctly reassigned to their a priori taxon, both overall and for each taxon separately. Because sexual dimorphism may affect multivariate cranial variation, we also tested the effects of species, sex, and their interaction using MANOVA on the same set of cranial variables included in the discriminant analyses. Specimens of indeterminate sex were excluded from this analysis. Multivariate significance was assessed using Pillai's trace. To analyze the data, two criteria were followed: The data were grouped according to the assignment to populations (nominal forms) obtained from the ancestry matrix and in the spatial domains of the *tess3r* analysis, based on the distribution ranges proposed by Novaes et al. [1] with comparative aims.

2.5 | Bioacoustic Analyses

Acoustic recordings used in the analyses came from the personal library of one of the authors (FL) and from other Chilean researchers and consisted of reference echolocation calls of *M. atacamensis* from the Arica and Parinacota regions in northernmost Chile. Following Novaes et al. [1], we assigned to *M. arescens* the calls recorded in central Chile with a FMaxE around 48

kHz and to *M. chiloensis* the calls recorded in southern Chile with a FMaxE around 45 kHz. Recordings of free-flying bats were obtained using an automatic recorder (Song Meter SM4BAT-FS, Wildlife Acoustics Inc., USA) with an external omnidirectional microphone placed at an approximate height of 2.5 m above ground level in uncluttered flyways, in both natural and anthropogenic habitats. Recorders ran for a minimum of one night at each site, from sunset to sunrise. Recordings were made using a sampling frequency of 256 kHz or higher.

For sound analysis, spectrograms were generated in Kaleidoscope (version 5.7.0, Wildlife Acoustics Inc., USA). For each echolocation sequence (defined as a recording file containing 6–10 pulses emitted by a bat), we obtained the following spectrographic variables, following Lisón [44] and Vilches-Piñones et al. [45]: start frequency (F_{start}), end frequency (F_{end}), frequency of maximum energy ($F_{Max,\ E}$), mean principal frequency ($F_{p,\ mean}$), call duration (D), and interpulse interval (IPI).

To determine whether echolocation calls could be separated into three independent groups corresponding to each taxon, we performed a discriminant function analysis (DFA) using the *MASS* and *lattice* package implemented in R [46, 47]. Wilks' λ values were obtained from a MANOVA to test the statistical significance of the DFA models, and differences were considered statistically significant when p-values were <0.05. Standardized discriminant function coefficients were used to determine the contribution that each variable made to the ability of the DFA to classify calls.

3 | Results

3.1 | Lineage Detection, Geographical Structure, and Genetic Diversity

Both exploratory multivariate and ancestry analyses revealed the presence of three well-defined genetic clusters among the studied specimens (Figure 1A, C). The overall genetic diversity of the putative species was lower than expected but remained well balanced between *M. arescens* and *M. chiloensis* (Table 1). Among the individuals originally assigned to *M. atacamensis* ($n = 9$), *M. arescens* ($n = 50$), and *M. chiloensis* ($n = 21$), the ancestry-based reassignment resulted in 5, 39, and 36 individuals, respectively, for each putative species (Table 1). This reclassification led to notable adjustments in the inferred limits of their distribution ranges: *M. atacamensis* extending southward up to 22°54′57″ S, *M. arescens* ranging from 27°04′58″ S to 35°24′50″ S, and *M. chiloensis* distributed between 36°16′58″ S and 54°28′35″ S (Figure 1B).

Furthermore, the genetic structure of these three groups exhibited a clear pattern of differentiation, with *M. atacamensis* markedly distinct from the remaining *Myotis* species in Chile (Figure 1A, C). As predicted, the putative species *M. arescens* and *M. chiloensis* displayed a latitudinal gradient of shared ancestry: Specimens from the extremes of their ranges were more differentiated, whereas those from south-central Chile showed a gradual admixture zone (Figure 1C). These findings are consistent with the estimated pairwise differentiation ($F_{ST} = 0.0688$, $p < 0.001$; Table 1), indicating limited but significant population structure between *M. arescens* and *M. chiloensis*. Coincidentally, the pattern detected by the Mantel test establishes that there is a very low but significant IBD, especially when comparing the forms *M. arescens* with *M. chiloensis* (Mantel $r = 0.121$; $p = 0.022$; Supporting Information 2: Figure S3).

Recent migration estimates further supported the distinctiveness of *M. atacamensis*, which exhibited no detectable gene flow with the other *Myotis* lineages in Chile. The few alleles shared between this species and the other nominal forms are therefore best explained by ancestral polymorphism rather than contemporary reproduction (Figure 1C). In contrast, migration rates between *M. arescens* and *M. chiloensis* were both significant and highly asymmetrical: Gene flow from *M. arescens* to *M. chiloensis* reached 7%, whereas the reverse direction attained 27% (Table 2). Hence, our results indicate predominant south-to-north gene flow among these two nominal forms of *Myotis*.

3.2 | Phylogeny and Species Delimitation Test

Phylogenetic reconstruction based on 19,707 SNPs provided strong support for the monophyly of *M. atacamensis*. However, no reciprocal monophyly was recovered between *M. arescens* and *M. chiloensis* (Figure 2). Among the five alternative models evaluated using the *delimitR* package [38], Model 2, which proposes deep divergence between *M. atacamensis* and the combined clade (*M. arescens* + *M. chiloensis*) but no differentiation within the latter, received the highest support (227 votes; posterior probability = 0.8822; Figure 2; Supporting Information 2: Figure S4).

TABLE 1 | Genetic diversity indices and pairwise population differentiation for the three focal *Myotis* species based on 19,707 SNPs.

					F_{st}	
Species	***n***	***H*$_o$**	***H*$_e$**	**F_{is}**	***M. atacamensis***	***M. arescens***
M. atacamensis	9	0.0385	0.1756	0.6474	—	
	5	0.0292	0.0566	0.3318		
M. arescens	50	0.0438	0.0758	0.3567	0.3792*	—
	39	0.0440	0.0751	0.3481	0.7587*	
M. chiloensis	21	0.0442	0.0736	0.3124	0.3672*	0.0572*
	36	0.0435	0.0741	0.3383	0.7611*	0.0688*

Note: For each taxon, the table reports sample size (n), observed heterozygosity (H_o), expected heterozygosity (H_e), inbreeding coefficient (F_{IS}), and pairwise F_{ST} values under two alternative population assignment scenarios: Upper values correspond to the arrangement of Novaes et al. [1], whereas lower values correspond to the ancestry-based assignment.
*p-Value < 0.001.

TABLE 2 | Migration matrix (migration rate and mean standard deviation) for the putative species of Chilean *Myotis*.

Species	*M. atacamensis*	*M. arescens*	*M. chiloensis*
M. atacamensis	0.9167 (0.0486)[a]	0.0411(0.0365)	0.0422 (0.0377)
M. arescens	0.0078 (0.0077)	0.9205 (0.0217)[a]	0.0717 (0.021)[a]
M. chiloensis	0.0085 (0.0084)	0.2725 (0.0210)[a]	0.719 (0.020)[a]

Note: Significance was assessed if 95% credible sets did not overlap with zero.
[a]Significant migration rate.

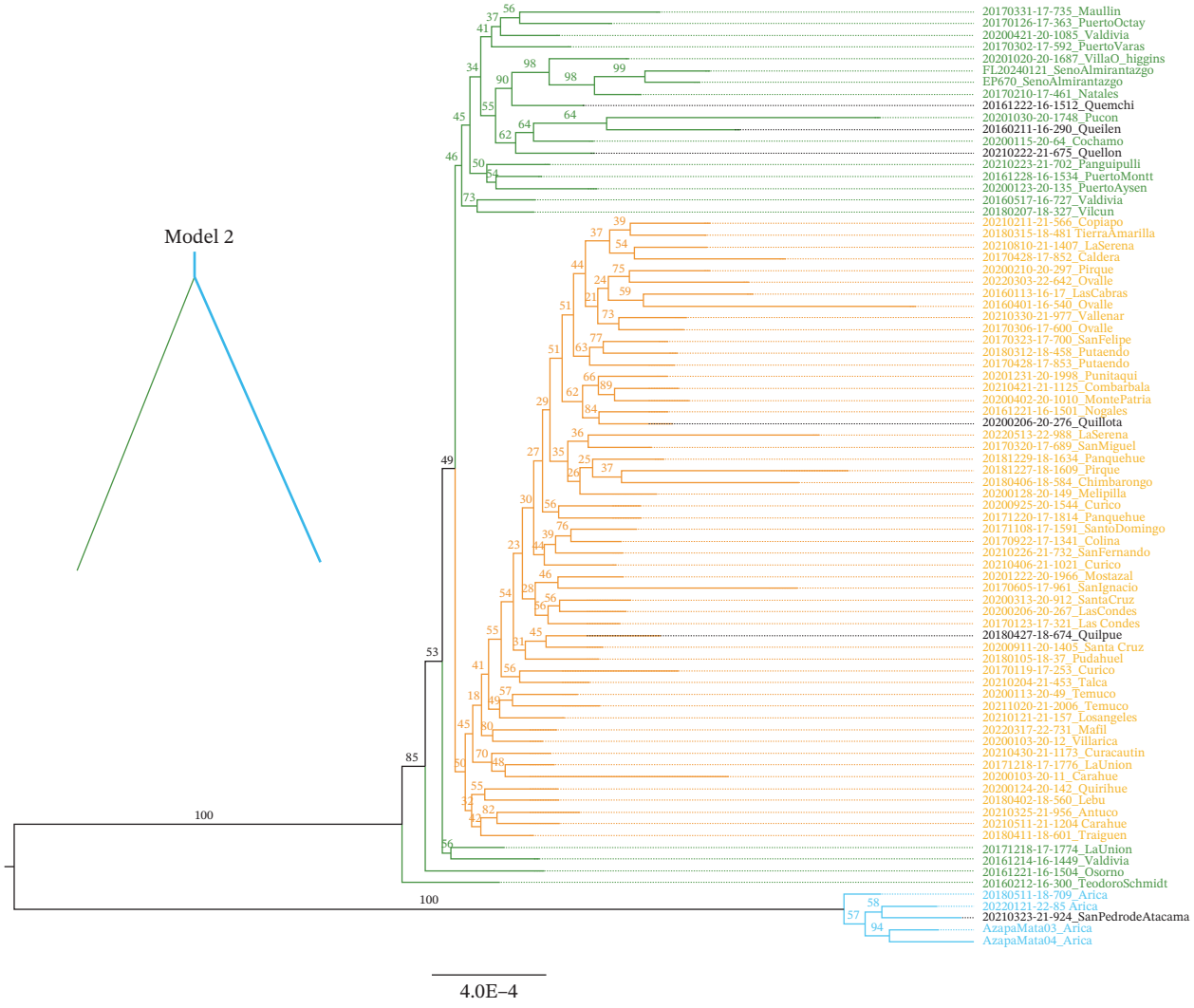

FIGURE 2 | Maximum likelihood phylogenetic relationships for Chilean *Myotis* specimens based on the molecular variation of SNPs. We included a topotype specimen for *M. atacamensis* (San Pedro de Atacama, Chile) and specimens for nearby localities of the types of *M. arescens* (type locality: Limache; close localities: Quilpué and Quillota) and *M. chiloensis* (type locality: islets on the eastern side of Chiloe Island; close localities and probably topotypes from: Quemchi, Queilén, and Quellón) but see LaVal [8]. The phylogeny strongly suggests two clades: *M. atacamensis* and *M. arescens* + *M. chiloensis*. The form *M. chiloensis* is polyphyletic under the scenario of valid *M. arescens*. Numbers on the branch reflect bootstrap support. Insert: *delimitR* result. The best model showed no divergence between *M. chiloensis* and *M. arescens*.

3.3 | Morphometric Analyses

All morphological traits analyzed showed pronounced differentiation in *M. atacamensis* compared to *M. arescens* and *M. chiloensis* (Table 3). This pattern was consistent whether specimens were classified according to the nominal distributions proposed by Novaes et al. [1] or reassigned based on genetic ancestry (Figure 3; Supporting Information 2: Figure S5). PCA revealed a clear separation of *M. atacamensis* along the first principal component (accounting for 68% of the total variance) and a slight

TABLE 3 | Body and craniodental measurements with their mean, maximum, minimum, and standard deviation for the 123 specimens of Chilean *Myotis*.

	Myotis atacamensis ($n = 6$)				*Myotis arescens* ($n = 66$)				*Myotis chiloensis* ($n = 51$)			
Trait	**Mean**	**Maximum**	**Minimum**	**SD**	**Mean**	**Maximum**	**Minimum**	**SD**	**Mean**	**Maximum**	**Minimum**	**SD**
FA	32.75	33.20	32.50	0.27	36.79	41.00	33.30	1.32	37.48	40.60	29.00	1.92
IOB	3.08	3.20	2.90	0.12	3.39	3.70	3.00	0.15	3.64	3.90	3.20	0.14
BAC	2.82	2.90	2.70	0.08	3.39	3.90	2.90	0.19	3.71	4.00	3.00	0.23
BAM	4.65	4.80	4.40	0.14	5.37	5.90	4.80	0.22	5.67	6.10	4.30	0.28
MTL	4.75	4.80	4.70	0.06	5.27	5.60	4.90	0.15	5.47	5.70	4.40	0.20
M1.3	2.83	3.00	2.70	0.12	3.15	3.90	2.90	0.14	3.23	3.40	3.00	0.10
HPC	2.45	2.70	2.30	0.14	3.00	3.50	2.40	0.20	3.21	3.70	2.30	0.26
LMD	9.10	9.20	8.90	0.11	10.04	10.70	9.30	0.28	10.50	11.30	9.40	0.38
Li1.M3	5.67	6.10	4.20	0.74	6.65	10.00	5.50	0.50	6.94	7.30	6.10	0.20
HMD	1.32	1.50	1.10	0.13	1.61	1.90	1.30	0.12	1.79	2.30	1.40	0.15

distinction along the second component (7%). In contrast, *M. arescens* and *M. chiloensis* exhibited substantial overlap. Notably, the highest loadings on PC1 corresponded to BAC (greatest breadth across outer edges of the crowns of upper canines, including cingulae) and LMD (Table 4), highlighting the marked differentiation of these cranial traits among the three nominal forms of Chilean *Myotis* (BAC: $F_{2,120} = 69.76$, $p < 0.001$; LMD: $F_{2,120} = 64.42$, $p < 0.001$). When maximizing between-group differences, the CDA revealed a similar pattern of separation (canonical root squares: 0.6719, approximate $F_{2,120} = 11.033$, $p < 0.001$; 0.2334, approximate $F_{2,120} = 3.7902$, $p = 0.003$; Figure 3). CDA indicated partial morphological separation among taxa, with most differentiation concentrated along the first canonical axis. LOOCV showed an overall classification success of 83.7%, with correct assignment rates of 86.4% for *M. arescens*, 100% for *M. atacamensis*, and 78.4% for *M. chiloensis*. Misclassifications occurred primarily between *M. arescens* and *M. chiloensis*, supporting the interpretation of partial morphological overlap between these taxa despite some separation in canonical space.

MANOVA excluding two specimens of indeterminate sex revealed a highly significant multivariate effect of species (Pillai's trace = 0.924, $p < 0.0001$) and a significant effect of sex (Pillai's trace = 0.276, $p = 0.0001$), whereas the species × sex interaction was not significant ($p = 0.742$). These results indicate that sexual dimorphism contributes to cranial variation but that its effect is broadly consistent across taxa and does not alter the main interspecific pattern.

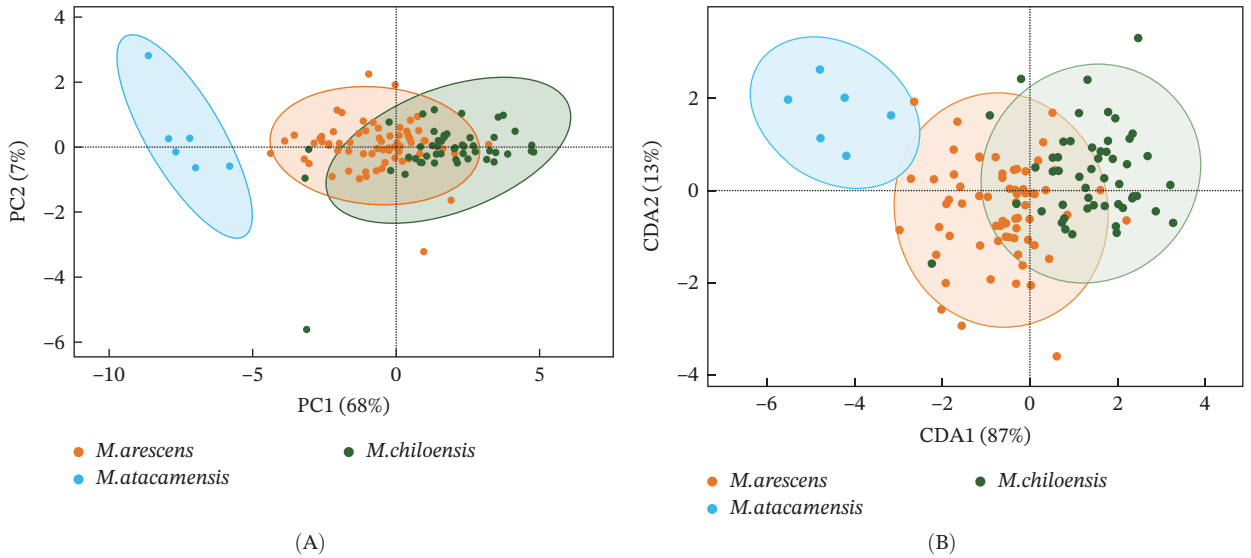

FIGURE 3 | Multivariate analysis of Chilean *Myotis* species. (A) Projections of scores for principal components PC1 and PC2, extracted from correlations of external and cranial measurements. (B) Canonical discriminant analysis (canonical scores) from correlations of external and cranial measurements. The data were grouped according to the assignment to populations (nominal forms) obtained from the ancestry matrix and in the spatial domains of the *tess3r* analysis.

TABLE 4 | Principal component eigenvalues, variance, and loadings based on morphological data for specimens of Chilean *Myotis*.

	Comp.1	Comp.2	Comp.3	Comp.4	Comp.5	Comp.6	Comp.7	Comp.8	Comp.9	Comp.10
Eigenvalues	2.602	0.843	0.772	0.747	0.625	0.586	0.510	0.394	0.348	0.302
Proportion of variance	0.677	0.071	0.060	0.056	0.039	0.034	0.026	0.016	0.012	0.009
Cumulative proportion	0.677	0.748	0.808	0.864	0.903	0.937	0.963	0.978	0.990	1.000
FA	0.271	0.029	0.678	0.598	0.058	0.227	0.080	0.216	0.032	0.020
IOB	0.331	−0.099	−0.014	−0.257	0.009	0.644	−0.426	−0.201	0.364	−0.215
BAC	0.354	0.136	−0.058	−0.283	−0.034	0.230	0.069	0.207	−0.236	0.784
BAM	0.339	0.353	−0.216	−0.131	−0.100	0.104	0.225	0.494	−0.283	−0.549
MTL	0.336	0.296	−0.171	0.111	−0.097	−0.101	0.568	−0.391	0.510	0.056
M1.3	0.304	−0.252	−0.183	0.263	−0.749	−0.269	−0.312	0.086	0.039	0.050
HPC	0.315	0.341	−0.043	0.037	0.456	−0.500	−0.502	0.140	0.222	0.049
LMD	0.356	0.041	0.170	−0.031	0.038	−0.129	−0.069	−0.647	−0.618	−0.136
Li1.M3	0.264	−0.568	−0.488	0.351	0.451	0.079	0.150	0.058	−0.105	0.007
HMD	0.274	−0.505	0.399	−0.522	0.042	−0.340	0.240	0.158	0.166	−0.106

3.4 | Bioacoustics Analyses

A total of 825 echolocation pulses (Table 5) were analyzed across the distribution ranges of the three species, following Novaes et al. [1]. Quantitative bioacoustic analyses distinguished the three taxa based on their echolocation calls. The multivariate DFA correctly classified 75.8% of the calls. MANOVA showed that the model was significant (Wilks' $\lambda = 0.482$, $F = 59.9$, and $p < 0.001$) and that 56.8% of the total acoustic variation was explained by the first discriminant function. The confusion matrix shows that calls of *M. atacamensis* are correctly identified in all cases, classification accuracy is high for *M. chiloensis* (87.0%), and calls of *M. arescens* are frequently confused with those of *M. chiloensis* (Table 6). The most important acoustic parameters for discrimination among these three taxa were end frequency (F_{end}), mean principal frequency ($F_{p,\ mean}$), and call duration (D). Overall, the DFA indicated that *M. arescens* cannot be acoustically separated from *M. chiloensis* based on their echolocation calls (Figure 4).

TABLE 6 | Confusion matrix of the echolocation call classification.

	Predicted		
Observed	***M. arescens***	***M. atacamensis***	***M. chiloensis***
M. arescens	190 (58.1%)	0 (0.0%)	137 (41.9%)
M. atacamensis	0 (0.0%)	14 (100.0%)	0 (0.0%)
M. chiloensis	61 (12.6%)	2 (0.4%)	421 (87.0%)

4 | Discussion

Our integrative analyses of genomic, bioacoustics, and morphometric data reveal a clear dichotomy in the evolutionary trajectories of Chilean *Myotis*. On one hand, *M. atacamensis* constitutes a deeply divergent lineage, genetically, bioacoustics, and morphologically distinct from all other taxa examined. On the otherhand, *M. arescens* emerges as a northern population embedded within the genetic and phenotypic continuum of *M. chiloensis*, with substantial asymmetric gene flow connecting both forms. This combination of sharp divergence in the north and gradual clinal variation southward suggests that distinct evolutionary processes shaped the diversification of *Myotis* across the latitudinal gradient of Chile.

4.1 | Taxonomic Implications and Lineage Distinctiveness

The strong genetic, bioacoustics, and morphological differentiation of *M. atacamensis* corroborates earlier phylogenomic

TABLE 5 | Descriptive statistics (mean ± SD [min–max]) of the echolocation calls (pulse type FM) of *M. atacamensis*, *M. arescens*, and *M. chiloensis*.

Species	*N*	F_{start}	F_{end}	$F_{Max,E}$	Duration	IPI	$F_{p,\ mean}$	Locality[a]
M. chiloensis	484	77.9 ± 9.6 [52.7–110.9]	37.2 ± 2.9 [24.2–43.9]	46.3 ± 2.5 [35.0–53.9]	6.9 ± 2.3 [1.9–13.1]	80.5 ± 29.1 [8.4–344.4]	48.1 ± 2.7 [37.7–58.2]	Temuco, Villarrica, Valdivia, Tierra del Fuego
M. arescens	327	79.7 ± 7.6 [58.4–103.3]	40.1 ± 2.4 [34.8–46.0]	49.0 ± 2.7 [45.0–64.0]	6.2 ± 2.1 [2.5–11.8]	70.7 ± 19.1 [26.7–135.2]	51.0 ± 2.7 [46.8–61.8]	Concepción, Maule, Santiago
M. atacamensis	14	112.6 ± 5.6 [100.5–119.5]	40.2 ± 1.4 [36.8–42.2]	47.8 ± 1.5 [46.6–51.7]	4.3 ± 0.6 [3.5–5.5]	81.4 ± 13.1 [54.4–98.1]	51.9 ± 2.4 [46.6–55.8]	Arica

[a]The spatial setting of these localities can be seen in Supporting Information 1: Table S1.

(A)

FIGURE 4 | (Continued)

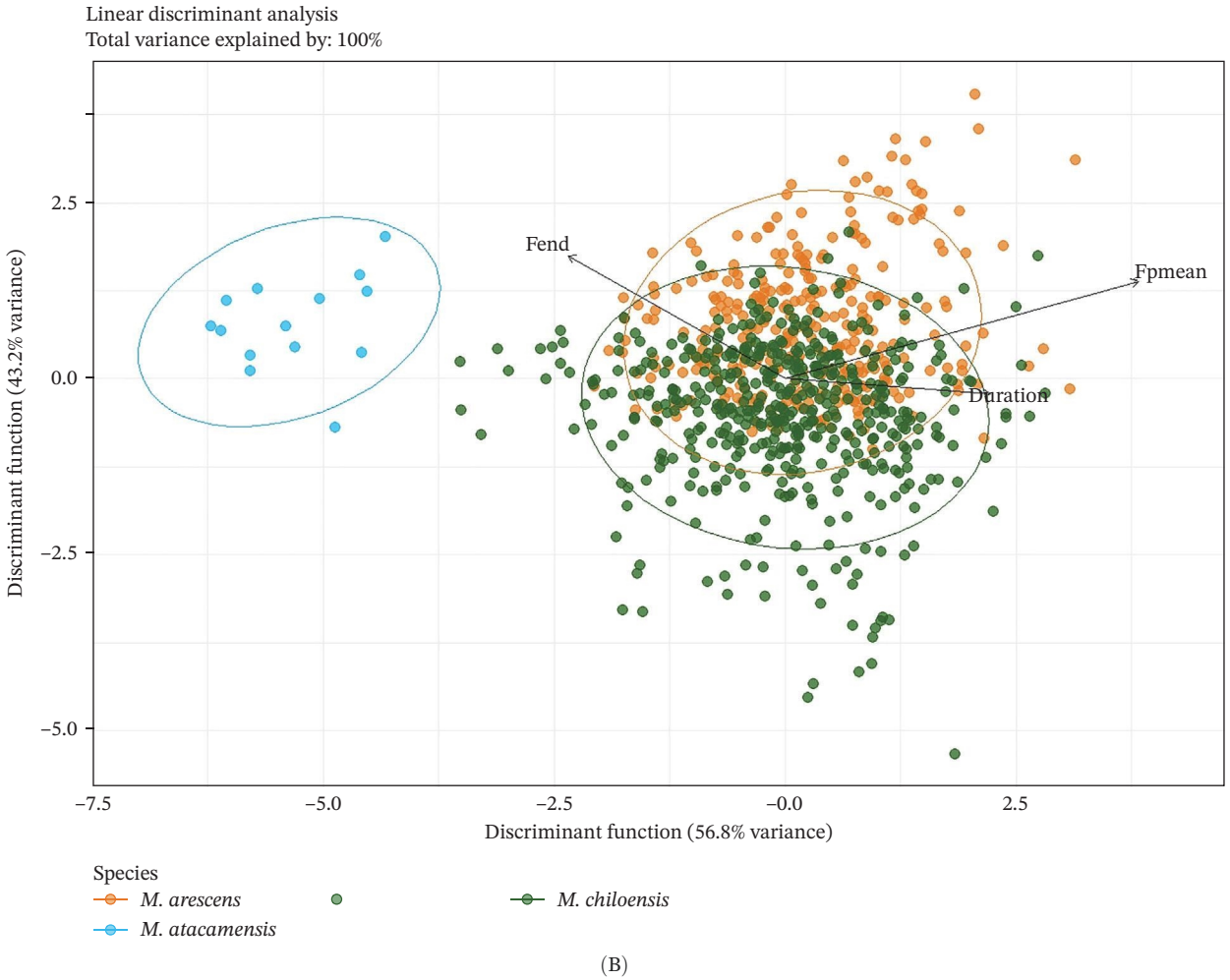

FIGURE 4 | Plots showing dispersion points and vector correlation of echolocation call measures of principal component analysis (A) and discriminant function analysis (B) for *Myotis* species from Chile.

findings based on ultraconserved elements [10] and supports its recognition as an independently evolving lineage. The absence of recent migration and the complete lack of admixture between northern (*M. atacamensis*) and southern taxa suggest the occurrence of reproductive isolation. Phylogenetically, *M. atacamensis* relates to Central American and arid–Andean taxa [3, 10], suggesting an ancient colonization of the hyperarid Atacama region, followed by long-term isolation. Morphologically, this species exhibits reduced cranial dimensions and toothrow lengths compared with southern congeners, consistent with the pattern observed in small-bodied, desert-adapted bats [48, 49]. The convergence between morphological and genomic datasets thus provides a robust basis for its species-level status under both evolutionary and operational criteria [50].

In contrast, the relationship between *M. arescens* and *M. chiloensis* appears better interpreted as a population-level differentiation within a single, geographically structured species. The lack of reciprocal monophyly, the low yet significant F_{ST} values, and the strong signal of asymmetric gene flow argue against complete isolation. Instead, these patterns reflect a continuum of divergence typical of populations connected by secondary contact or incomplete lineage sorting [51, 52]. Our results are therefore more consistent with *M. arescens* representing a northern quite subtle morphotype of *M. chiloensis* rather than a distinct species. For this reason, and in agreement with the original treatment of Osgood [7], we consider the most appropriate interpretation to be retention as a subspecies, *M. c. arescens*, rather than recognition as a full species.

4.2 | Patterns of Gene Flow and Isolation

The asymmetric migration detected between *M. chiloensis* and *M. arescens* (27% northward vs. 7% southward) is consistent with spatially structured contemporary gene flow across a clinal contact zone. Because these estimates were obtained with BayesAss3-SNPs, they should be interpreted as reflecting recent migration rather than deep historical introgression. In this context, the clinal admixture recovered by sNMF, together with the low but significant IBD pattern indicated by the Mantel test, supports the view that these nominal forms remain connected by ongoing gene flow across a geographically continuous range. Such asymmetric contemporary gene flow may arise under range-expansion scenarios but can also occur in other demographic contexts, including secondary contact and spatially heterogeneous connectivity [53, 54].

Although the observed asymmetry does not by itself demonstrate postglacial recolonization, it is compatible with a broader biogeographic scenario in which south-to-north range shifts following the Last Glacial Maximum (LGM) contributed to the present spatial structure of variation in *M. chiloensis*. Paleoclimatic reconstructions indicate that mesic vegetation belts expanded northward in Chile after the LGM, potentially facilitating range connectivity and progressive recolonization across central Chile [55–57]. Under this interpretation, the current pattern of asymmetric migration may represent the demographic legacy of historical range dynamics superimposed on ongoing connectivity and local differentiation. At the same time, this scenario should be viewed as a biogeographic hypothesis consistent with the spatial genetic pattern rather than as a direct demographic inference. The slightly higher genetic diversity observed in *M. arescens* could also be compatible with the retention of ancestral polymorphisms or persistence in climatically transitional refugial areas during glacial cycles.

This demographic and environmental context helps explain why genetic, bioacoustic, and morphological discontinuities are weak between *M. chiloensis* and *M. arescens*. The moderate but significant F_{ST} value (0.0688) and the overlap in multivariate morphometric space are more consistent with structured populations connected by gene flow than with fully distinct evolutionary species [58, 59]. The lack of strong ecological or geographic barriers across their ranges further supports this interpretation. Both taxa occupy contiguous areas characterized by relatively continuous forest and shrubland mosaics, with no obvious break likely to promote speciation through ecological segregation. The apparent morphological shift toward smaller cranial proportions in *M. arescens* may therefore reflect local differentiation along environmental gradients rather than speciation sensu stricto.

4.3 | Morphological Variation and Functional Implications

The morphometric analyses reinforce the genomic inference of population-level differentiation. While *M. atacamensis* shows pronounced cranial reduction, *M. arescens* and *M. chiloensis* differ mainly along size gradients, particularly in traits associated with bite force and feeding mechanics (e.g., BAC and LMD). Such variation may reflect adaptive responses to latitudinal changes in prey availability, habitat use, and climatic constraints [45, 60, 61]. The overlap between *M. arescens* and *M. chiloensis* in both PCA and CDA suggests that morphological divergence remains insufficient to produce diagnostic characters, in contrast with the sharp morphometric boundaries observed in *M. atacamensis*. Similar patterns of subtle cranial gradients have been reported in other Neotropical *Myotis*, such as *M. nigricans* and *M. albescens*, where intraspecific geographic variation parallels environmental clines rather than lineage divergence [62, 63]. Hence, the morphological continuum observed here provides further evidence against the recognition of *M. arescens* as a separate species.

Importantly, this result does not diminish the ecological or evolutionary significance of the northern populations. Instead, *M. arescens* may represent a population maintaining substantial gene flow yet experiencing local selective pressures. Peripheral or climatic differentiated populations often contribute disproportionately to evolutionary innovation and resilience, acting as sources of adaptive variation [64, 65]. Therefore, understanding the ecological differentiation within *M. chiloensis* could be critical for conserving adaptive potential across the species' latitudinal range.

4.4 | Historical Biogeographic Context

The estimated divergence between *M. atacamensis* and the clade that includes *M. chiloensis* at ~11.8 Ma [10] coincides with major Andean uplift events and the onset of hyperaridity in northern Chile [66, 67]. These processes likely produced the ecological isolation necessary for the early divergence of *M. atacamensis* with respect to other congeneric Neotropical lineages. In contrast, the diversification within *M. chiloensis* appears to be much more recent and spatially diffuse, occurring along the continuous temperate corridor of central and southern Chile. The absence of deep phylogenetic breaks within this lineage is consistent with postglacial range shifts along this corridor, as observed in other vertebrates with similar distributions, including sigmodontine rodents (*Oligoryzomys longicaudatus* and *Abrothrix olivacea*; [68, 69]) and marsupials (*Thylamys elegans*; [70]). Such congruent patterns suggest a shared history of latitudinal connectivity and demographic expansion rather than repeated speciation events.

From a broader Neotropical perspective, our results emphasize that morphological conservatism within *Myotis* can mask significant phylogeographic structure. However, not all genetic structuring equates to species-level divergence. Distinguishing between population structure and speciation requires explicit modeling of gene flow and demography, as implemented here. In this sense, integrative frameworks combining genome-wide SNP data, morphology, bioacoustics, and spatial modeling provide a more nuanced view of lineage boundaries than traditional taxonomic approaches [20, 71].

4.5 | Revisiting Species Delimitation in Chilean and Neotropical *Myotis*

The process-based analysis implemented in *delimitR* provided quantitative support for a two-lineage model in Chilean *Myotis*: one corresponding to *M. atacamensis* and another encompassing *M. chiloensis* plus *M. arescens*. This model best fits the data because it allows gene flow within the southern clade while maintaining strong divergence from the northern species. The agreement between this result and both phylogenomic and morphometric patterns strengthens the inference of population connectivity within the *M. chiloensis* complex. Moreover, it illustrates the value of model-based delimitation methods that incorporate population processes, avoiding the taxonomic inflation often produced by purely tree-based approaches [38, 71]. Consequently, we propose retaining only two species of *Myotis* in Chile: *M. atacamensis* and *M. chiloensis*, the latter including the populations historically referred to as *M. arescens*. Within *M. chiloensis*, genetic and morphological gradients indicate population structuring that likely reflects environmental and recent-historical influences rather than speciation. Recognizing this hierarchical structure (species, subspecies, and population) provides a biologically meaningful taxonomy consistent with both evolutionary processes and conservation priorities.

The discrepancy between our conclusions and those of Novaes et al. [1] may be explained, at least in part, by differences in sampling design. In Novaes et al. [1], the specimens included in both the genetic and morphological analyses were drawn largely from the geographic extremes of the distribution of the nominal forms within the *M. chiloensis* complex. In a system characterized by clinal genetic structure and gradual morphological differentiation, such a design is likely to maximize apparent divergence by emphasizing the most contrasting populations while underrepresenting intermediate populations. In addition, the discrepancy between previous mitochondrial results and our nuclear SNP data may also reflect the different evolutionary properties of these marker systems. Because mitochondrial DNA represents a single, maternally inherited locus with a smaller effective population size, it may show stronger geographic structure or retain signals of historical isolation even when contemporary nuclear gene flow is present. Processes such as incomplete lineage sorting or mitochondrial introgression could therefore contribute to a stronger pattern of mitochondrial divergence than is recovered from genome-wide nuclear data.

More broadly, our results highlight the value of integrative frameworks for resolving taxonomic controversies in Neotropical Myotinae. Comparable challenges have been documented in other *Myotis* lineages, including the *M. nigricans* complex and the *M. oxyotus* group, where cryptic diversity, limited phenotypic differentiation, and conflicting molecular signals have complicated species delimitation. In this context, our combination of model-based delimitation, explicit inference of recent asymmetric gene flow, and geographically dense sampling provides a useful framework for evaluating lineage limits in systems where clinal variation, introgression, and incomplete lineage sorting may otherwise obscure taxonomic boundaries. More generally, because mitonuclear discordance appears to be widespread in *Myotis*, integrative approaches of this kind may be especially important for avoiding both taxonomic oversplitting and the underrecognition of independently evolving lineages [72–74].

4.6 | Limitations and Future Directions

Despite the comprehensive nature of our dataset, some limitations remain. Sampling in northernmost and southernmost localities is still sparse, potentially underrepresenting the full extent of contact zones or cryptic diversity. Indeed, a more comprehensive understanding of the evolutionary history of *M. chiloensis* in southern South America also requires taking into account a substantial part of its distribution in southern Argentina. Moreover, while genome-wide SNPs provide excellent resolution for recent divergences, they offer limited information on historical demography and past hybridization. Integrating these data with coalescent-based demographic models (e.g., G-PhoCS and MSMC; [75, 76]) or whole-genome sequences would refine estimates of divergence times and migration rates. Similarly, expanding bioacoustic analyses (which remain underexplored in this complex) could reveal additional behavioral differentiation correlated with genetic structure. Acoustic traits, such as call frequency and duration, often evolve rapidly and can contribute to reproductive isolation in bats [77, 78].

5 | Conclusions

Taken together, our results show that the evolutionary history of Chilean *Myotis* reflects a mixture of ancient isolation and recent connectivity. *M. atacamensis* represents an arid-adapted relict lineage whose long-term separation from southern congeners justifies its recognition as a distinct species. In contrast, *M. arescens* and *M. chiloensis* form a single, geographically structured lineage shaped by historical range dynamics and ongoing gene flow. This pattern underscores the importance of viewing species boundaries as dynamic, process-driven outcomes rather than purely divergence-supported entities. By integrating genomic, morphological, bioacoustics, and spatial evidence, our study resolves a long-standing taxonomic debate and provides a framework for interpreting intraspecific variation in cryptic bat taxa. More broadly, it illustrates how population connectivity and local adaptation can coexist within morphologically conserved lineages, shaping biodiversity patterns across environmental gradients. Future work combining genomics, bioacoustics, and ecological modeling will be key to further disentangling the complex evolutionary history of *Myotis* in southern South America.

Acknowledgments

We thank Verónica Jung and Instituto de Salud Pública del Ministerio de Salud del Gobierno de Chile (ISPCh) for providing some bat specimens for analysis. We are also grateful to Gonzalo Ossa and Karol Ida Vilches-Piñones for sharing echolocation sound files of *Myotis* species collected across Chile. We are deeply grateful for the solid, constructive, and detailed insights made by two anonymous reviewers. Financial support was provided by the Agencia Nacional de Investigación y Desarrollo del Gobierno de Chile (FONDECYT Grants 1220998 and 1240219) and the "Subprograma Regional Saavedra Fajardo de la Fundación Séneca—Agencia de Ciencia y Tecnología de la Región de Murcia" (FS/10.13039/100007801 [Grant 22829/SF/24]).

Funding

Financial support was provided by the Fondo Nacional de Desarrollo Científico y Tecnológico (FONDECYT Grants 1220998 and 1240219) and the "Subprograma Regional Saavedra Fajardo de la Fundación Séneca—Agencia de Ciencia y Tecnología de la Región de Murcia" (FS/10.13039/100007801 [Grant 22829/SF/24]).

Conflicts of Interest

The authors declare no conflicts of interest.

Data Availability Statement

All data generated and analyzed during this study are included in the Supporting Information files and are also publicly available through Zenodo at https://doi.org/10.5281/zenodo.18237366.

References

1. R. L. M. Novaes, A. Rodriguez-San Pedro, M. M. Saldarriaga-Cordoba, O. Aguilera-Acuna, D. Wilson, and R. Moratelli, "Systematic Review of *Myotis* (Chiroptera, Vespertilionidae) From Chile Based on Molecular, Morphological, and Bioacoustic Data," *Zootaxa* 5188, no. 5 (2022): 430–452.

2. S. M. Ospina-Garcés, J. Arroyo-Cabrales, and R. A. Medellín, "Cranial Morphology of the Flat-Headed Bat *Myotis planiceps* (Chiroptera:

Vespertilionidae) in the Context of American *Myotis*," *Acta Chiropterologica* 23, no. 1 (2021): 45–58.

3. R. J. Larsen, M. C. Knapp, H. H. Genoways, et al., "Genetic Diversity of Neotropical *Myotis* (Chiroptera: Vespertilionidae) With an Emphasis on South American Species," *PLOS ONE* 7, no. 10 (2012): e46578.

4. A. Cabrera, "Catálogo descriptivo de los quirópteros chilenos," *Revista Chilena de Historia Natural* 7, no. 5-6 (1903): 278–308.

5. G. Waterhouse and C. Darwin, *The Zoology of the Voyage of the H. M. S. Beagle (Part II, Mammalia)* (Smith, Elder and Co, 1839): 1–97.

6. F. Lataste, "Études sur faune chilienne. II—Note sur les chauve-souris (Ordre des Chiroptères)," *Actes de la Société Scientifique du Chile* 1 (1891): 70–91.

7. W. H. Osgood, *The Mammals of Chile* (Field Museum of Natural History, 1943).

8. R. K. LaVal, "A Revision of the Neotropical Bats of the Genus *Myotis*," *Contributions in Science* 15 (1973): 1–54.

9. G. Mann, "Los pequeños mamíferos de Chile," *Gayana* 40 (1978): 1–342.

10. A. E. Morales, M. Ruedi, K. Field, and B. C. Carstens, "Diversification Rates Have No Effect on the Convergent Evolution of Foraging Strategies in the Most Speciose Genus of Bats, *Myotis*," *Evolution* 73, no. 11 (2019): 2263–2280.

11. A. L. Gardner, "Volume 1: Marsupials, Xenarthrans, Shrews, and Bats," in *Mammals of South America*, (University of Chicago Press, 2007).

12. M. Canals and P. Cattan, *Murciélagos de Chile: Radiografía a los murciélagos de chile* (Editorial Universitaria, 2008).

13. A. Iriarte, *Mamíferos de Chile* (Lynx Editions, 2008).

14. D. E. Wilson, "Genus *Myotis*," in *Mammals of South America. Volume 1: Marsupials, Xenarthrans, Shrews, and Bats*, ed. A. L. Gardner, (University of Chicago Press, 2008): 468–481.

15. G. Ossa and A. Rodríguez-San Pedro, "*Myotis chiloensis* (Chiroptera: Vespertilionidae)," *Mammalian Species* 47, no. 922 (2015): 51–56.

16. R. L. M. Novaes, D. E. Wilson, M. Ruedi, and R. Moratelli, "The Taxonomic Status of *Myotis aelleni* Baud, 1979 (Chiroptera, Vespertilionidae)," *Zootaxa* 4446, no. 2 (2018): 257–264.

17. R. Moratelli, R. L. M. Novaes, C. Carrión-Bonilla, et al., *A New Species of Myotis (Chiroptera, Vespertilionidae) From Peru* (Special Publications of the Museum of Texas Tech University, 2019): 239–256.

18. B. K. Peterson, J. N. Weber, E. H. Kay, H. S. Fisher, and H. E. Hoekstra, "Double Digest RADseq: An Inexpensive Method for de Novo SNP Discovery and Genotyping in Model and Non-Model Species," *PLOS ONE* 7, no. 5 (2012): e37135.

19. K. R. Andrews, J. M. Good, M. R. Miller, G. Luikart, and P. A. Hohenlohe, "Harnessing the Power of RADseq for Ecological and Evolutionary Genomics," *Nature Reviews Genetics* 17, no. 2 (2016): 81–92.

20. B. C. Carstens, T. A. Pelletier, N. M. Reid, and J. D. Satler, "How to Fail at Species Delimitation," *Molecular Ecology* 22, no. 17 (2013): 4369–4383.

21. J. M. Korstian, N. S. Paulat, R. N. Platt II, R. D. Stevens, and D. A. Ray, "SINE-Based Phylogenomics Reveal Extensive Introgression and Incomplete Lineage Sorting in *Myotis*," *Genes* 13, no. 3 (2022): 399.

22. A. E. Morales and B. C. Carstens, "Evidence that *Myotis lucifugus* "Subspecies" are Five Nonsister Species, Despite Gene Flow," *Systematic Biology* 67, no. 5 (2018): 756–769.

23. D. Josić, E. Çoraman, I. Waurick, et al., "Cryptic Hybridization Between the Ancient Lineages of Natterer's Bat (*Myotis nattereri*)," *Molecular Ecology* 33, no. 13 (2024): e17411.

24. A. Kilian, P. Wenzl, E. Huttner, et al., "Diversity Arrays Technology: A Generic Genome Profiling Technology on Open Platforms," *Methods in Molecular Biology* 888 (2012): 67–89.

25. N. S. Paulat, J. M. Storer, D. D. Moreno-Santillán, et al., "Chiropterans are a Hotspot for Horizontal Transfer of DNA Transposons in Mammalia," *Molecular Biology and Evolution* 40, no. 5 (2023): msad092.

26. J. N. Curti, D. Fraser, M. Escalona, et al., "A Genome Assembly of the Yuma Myotis Bat, *Myotis yumanensis*," *Journal of Heredity* 115, no. 1 (2024): 139–148.

27. B. S. Weir and C. C. Cockerham, "Estimating F-Statistics for the Analysis of Population Structure," *Evolution* 38, no. 6 (1984): 1358–1370.

28. Z. N. Kamvar, J. C. Brooks, and N. J. Grünwald, "Novel R Tools for Analysis of Genome-Wide Population Genetic Data With Emphasis on Clonality," *Frontiers in Genetics* 6 (2015): 208.

29. Z. N. Kamvar, J. F. Tabima, and N. J. Grünwald, "Poppr: An R Package for Genetic Analysis of Populations With Clonal, Partially Clonal, and/or Sexual Reproduction," *PeerJ* 2 (2014): e281.

30. R. J. Hijmans, "*Geosphere: Spherical Trigonometry* (R Package Version 1.5-18)," 2023, https://CRAN.R-project.org/package=geosphere.

31. J. Oksanen, G. Simpson, F. Blanchet, et al., "*Vegan: Community Ecology Package* (R Package Version 2.8-0)," 2025, https://vegandevs.github.io/vegan/.

32. E. Frichot and O. François, "LEA: An R Package for Landscape and Ecological Association Studies," *Methods in Ecology and Evolution* 6, no. 8 (2015): 925–929.

33. K. Caye, T. M. Deist, H. Martins, O. Michel, and O. François, "TESS3: Fast Inference of Spatial Population Structure and Genome Scans for Selection," *Molecular Ecology Resources* 16, no. 2 (2016): 540–548.

34. S. M. Mussmann, M. R. Douglas, T. K. Chafin, and M. E. Douglas, "BA3-SNPs: Contemporary Migration Reconfigured in BayesAss for Next-Generation Sequence Data," *Methods in Ecology and Evolution* 10, no. 10 (2019): 1808–1813.

35. G. A. Wilson and B. Rannala, "Bayesian Inference of Recent Migration Rates Using Multilocus Genotypes," *Genetics* 163, no. 3 (2003): 1177–1191.

36. A. Rambaut, A. J. Drummond, D. Xie, G. Baele, and M. A. Suchard, "Posterior Summarisation in Bayesian Phylogenetics Using Tracer 1.7," *Systematic Biology* 67, no. 5 (2018): 901–904.

37. T. K. F. Wong, N. Ly-Trong, H. Ren, et al., "IQ-TREE. 3: Phylogenomic Inference Software Using Complex Evolutionary Models," *Preprint/Submitted Manuscript* (2025).

38. M. L. Smith and B. C. Carstens, "Process-Based Species Delimitation Leads to Identification of More Biologically Relevant Species," *Evolution* 74, no. 2 (2019): 216–229.

39. F. Di Castri and E. Hajek, *Bioclimatología de Chile* (Universidad Católica de Chile, 1976).

40. Y. Bhak, Y. Jeon, S. Jeon, et al., "*Myotis rufoniger* Genome Sequence and Analyses: *M. rufoniger*'s Genomic Feature and the Decreasing Effective Population Size of *Myotis* Bats," *PLOS ONE* 12, no. 7 (2017): e0180418.

41. I. Horáček, W. Bogdanowicz, and B. Dulić, "*Plecotus austriacus* (Fisher, 1826)–Graues Langohr," in *Handbuch der Säugetiere Europas. Fledertiere II*, eds. J. Niethammer and F. Krapp, (Aula-Verlag, 2004).

42. R Core Team, *R: A Language and Environment for Statistical Computing* (R Foundation for Statistical Computing, 2025).

43. M. Friendly and J. Fox, "*Candisc: Visualizing Generalized Canonical Discriminant and Canonical Correlation Analysis* (R Package Version 0.9-3)," 2025, https://CRAN.R-project.org/package=candisc.

44. F. Lisón, "Clave de identificación para las llamadas de ecolocalización de los murciélagos de la Península Ibérica," (2011).

45. K. Vilches-Piñones, C. Matus-Olivares, G. Catalán, and F. Lisón, "Effect of Forest Areas Configuration on the Community of Insectivorous Bats in Agroforestry Landscapes," *Austral Ecology* 49, no. 2 (2024): e13268.

46. W. N. Venables and B. D. Ripley, *Modern Applied Statistics With S*, 4 ed. (Springer, 2002).

47. D. Sarkar, *Lattice: Multivariate Data Visualization With R* (Springer, 2008).

48. U. M. Norberg and J. M. V. Rayner, "Ecological Morphology and Flight in Bats (Mammalia; Chiroptera): Wing Adaptations, Flight Performance, Foraging Strategy and Echolocation," *Philosophical Transactions of the Royal Society of London. Series B, Biological Sciences* 316, no. 1179 (1987): 335–427.

49. I. Conenna, A. Muñoz-García, and C. Korine, "Physiological and Behavioural Strategies of Bats From Arid Environments," *Mammal Review* 55, no. 4 (2025): e70005.

50. K. De Queiroz, "Species Concepts and Species Delimitation," *Systematic Biology* 56 (2007): 879–886.

51. J. L. Feder, S. P. Egan, and P. Nosil, "The Genomics of Speciation-With-Gene-Flow," *Trends in Genetics* 28, no. 7 (2012): 342–350.

52. C. Roux, C. Fraïsse, J. Romiguier, Y. Anciaux, N. Galtier, and N. Bierne, "Shedding Light on the Grey Zone of Speciation Along a Continuum of Genomic Divergence," *PLOS Biology* 14, no. 12 (2016): e2000234.

53. L. Excoffier, M. Foll, and R. J. Petit, "Genetic Consequences of Range Expansions," *Annual Review of Ecology, Evolution, and Systematics* 40 (2009): 481–501.

54. A. W. Nolte, Z. Gompert, and C. A. Buerkle, "Variable Patterns of Introgression in Two Sculpin Hybrid Zones Suggest that Genomic Isolation Differs Among Populations," *Molecular Ecology* 18, no. 12 (2009): 2615–2627.

55. C. Villagrán and L. F. Hinojosa, "Historia de los bosques del sur de Sudamérica. II: Análisis fitogeográfico," *Revista Chilena de Historia Natural* 70 (1997): 241–267.

56. C. Villagrán, C. Le-Quesne, J. C. Aravena, H. Jiménez, and F. Hinojosa, "El rol de los cambios de clima del cuaternario en la distribución actual de la vegetación de Chile central-sur," *Bamberger Geographische Schriften* 15 (1998): 227–242.

57. F. Leubert and M. Weigend, "Phylogenetic Insights Into Andean Plant Diversification," *Frontiers in Ecology and Evolution* 2 (2014): 27.

58. C. Moritz, "Defining "Evolutionarily Significant Units" for Conservation," *Trends in Ecology & Evolution* 9, no. 10 (1994): 373–375.

59. C. Pinho and J. Hey, "Divergence With Gene Flow: Models and Data," *Annual Review of Ecology, Evolution, and Systematics* 41, no. 1 (2010): 215–230.

60. L. F. Aguirre, A. Herrel, R. Van Damme, and E. Matthysen, "The Implications of Food Hardness for Diet in Bats," *Functional Ecology* 17, no. 2 (2003): 201–212.

61. S. E. Santana, E. R. Dumont, and J. L. Davis, "Mechanics of Bite Force Production and Its Relationship to Diet in Bats," *Functional Ecology* 24, no. 4 (2010): 776–784.

62. R. Moratelli and J. A. de Oliveira, "Morphometric and Morphological Variation in South American Populations of *Myotis albescens* (Chiroptera: Vespertilionidae)," *Zoologia* 28, no. 6 (2011): 789–802.

63. R. Moratelli, A. L. Peracchi, D. Dias, and J. A. de Oliveira, "Geographic Variation in South American Populations of *Myotis nigricans* (Schinz, 1821) (Chiroptera, Vespertilionidae), With the Description of Two New Species," *Mammalian Biology* 76, no. 5 (2011): 592–607.

64. P. Lesica and F. W. Allendorf, "When are Peripheral Populations Valuable for Conservation?" *Conservation Biology* 9, no. 4 (1995): 753–760.

65. J. P. Sexton, P. J. McIntyre, A. L. Angert, and K. J. Rice, "Evolution and Ecology of Species Range Limits," *Annual Review of Ecology, Evolution, and Systematics* 40, no. 1 (2009): 415–436.

66. J. Houston and A. J. Hartley, "The Central Andean West-Slope Rainshadow and Its Potential Contribution to the Origin of Hyper-Aridity in the Atacama Desert," *International Journal of Climatology* 23, no. 12 (2003): 1453–1464.

67. A. J. Hartley, G. Chong, J. Houston, and A. E. Mather, "150 Million Years of Climatic Stability: Evidence From the Atacama Desert, Northern Chile," *Journal of the Geological Society* 162, no. 3 (2005): 421–424.

68. R. E. Palma, D. Boric-Bargetto, F. Torres-Pérez, C. E. Hernández, and T. L. Yates, "Glaciation Effects on the Phylogeographic Structure of *Oligoryzomys longicaudatus* (Rodentia: Sigmodontinae) in the Southern Andes," *PLOS ONE* 7, no. 3 (2012): e32206.

69. E. Rodríguez-Serrano, R. Cancino, and R. E. Palma, "Molecular Phylogeography of *Abrothrix olivaceus* (Rodentia: Sigmodontinae) in Chile," *Journal of Mammalogy* 87, no. 5 (2006): 971–980.

70. D. Boric-Bargetto, Á. Zúñiga-Reinoso, O. Inostroza-Michel, et al., "A Comprehensive Overview of the Genetic Diversity in *Thylamys elegans* (Didelphimorphia: Didelphidae): Establishing the Phylogeographic Determinants," *Revista Chilena De Historia Natural* 94, no. 1 (2021): 5.

71. J. Sukumaran and L. L. Knowles, "Multispecies Coalescent Delimits Structure, Not Species," *Proceedings of the National Academy of Sciences of the United States of America* 114, no. 7 (2017): 1607–1612.

72. R. N. Platt II, B. C. Faircloth, K. A. M. Sullivan, et al., "Conflicting Evolutionary Histories of the Mitochondrial and Nuclear Genomes in New World *Myotis*," *Systematic Biology* 67, no. 2 (2018): 236–249.

73. R. L. M. Novaes, V. C. Cláudio, D. E. Wilson, M. Weksler, and R. Moratelli, "Taxonomic Status of *Myotis Extremus* (Chiroptera, Vespertilionidae) From Mesoamerica, With Comments on the Distribution and Systematics of *Myotis nigricans*," *Zoologischer Anzeiger* 308 (2024): 99–110.

74. R. L. M. Novaes, C. E. Medina, S. Arias, D. E. Wilson, and R. Moratelli, "Unveiling the Shelf Life: A New Cryptic Species of *Myotis* (Chiroptera, Vespertilionidae) From South America Revealed by an Integrative Taxonomy Approach," *Journal of Mammalogy* 106, no. 4 (2025): 878–897.

75. I. Gronau, M. J. Hubisz, B. Gulko, C. G. Danko, and A. Siepel, "Bayesian Inference of Ancient Human Demography From Individual Genome Sequences," *Nature Genetics* 43, no. 10 (2011): 1031–1034.

76. S. Schiffels and R. Durbin, "Inferring Human Population Size and Separation History From Multiple Genome Sequences," *Nature Genetics* 46, no. 8 (2014): 919–925.

77. T. Kingston and S. J. Rossiter, "Harmonic-Hopping in Wallacea's Bats," *Nature* 429, no. 6992 (2004): 654–657.

78. D. S. Jacobs, S. Catto, G. L. Mutumi, N. Finger, and P. W. Webala, "Testing the Sensory Drive Hypothesis: Geographic Variation in Echolocation Frequencies of Geoffroy's Horseshoe Bat (Rhinolophidae: *Rhinolophus clivosus*)," *PLOS ONE* 12, no. 11 (2017): e0187769.

Supporting Information

Additional supporting information can be found online in the Supporting Information section. **Supporting Information 1**. Table S1: An Excel file.

Supporting Information 2. Word document with descriptions of Tables S1 and S2 (which provide details of the specimens used to obtain the genotypes and morphological data) and the STROBE Statement–Checklist. This document also includes all supporting figures and their captions (Figure S1–S5). **Supporting Information 3**. Table S2: An Excel file. **Supporting Information 4**. STROBE Statement—Checklist of items that should be included in reports of cross-sectional studies.